A Water Tank Prototype for the Cerenkov Calorimeter*

CHEN Ming-Jun[1,2;1)] WANG Yi-Fang[1] HE Jing-Tang[1] MENG Xiang-Cheng[1]
YU Mei-Ling[1] YANG Chang-Gen[1] CAO Jun[1]

1 (Institute of High Energy Physics, CAS, Beijing 100049, China)
2 (University of Science and Technology of China, Hefei 230026, China)

Abstract The water tank prototype with a dimension of 1m × 1m × 13m was constructed as a building block of the Cerenkov calorimeter for very long baseline neutrino oscillation experiments. The effective attenuation length of the water tank was measured to be (5.74±0.29)m, and the light collection probability as a function of the incident angle of the particle is studied. Results are compared with a Monte Carlo simulation based on GEANT4 package which incorporates detailed optical processes. A good agreement is achieved and the water tank is feasible for the construction of the Cerenkov calorimeter.

Key words neutrino, oscillation, detector, calorimeter

1 Introduction

Water is one of the most economic materials for large scale neutrino detectors. Water Cerenkov ring image detectors have been successfully employed in large scale experiments such as Super-Kamiokande[1], MiniBooNE[2] and IMB[3], etc. However such kind of detectors are not suitable for neutrinos with an energy more than ~4GeV due to complications of showers, therefore they are not the choice for very long baseline neutrino oscillation experiments. Water Cerenkov calorimeter[4], made up by a matrix of water tanks, is similar in a sense to the crystal calorimeter in accelerator experiments. Cerenkov light produced in the water tank is sufficient to have a good energy resolution, and the event pattern of the energy deposit in the water tank matrix can be used to identify neutrinos undergoing charge current interactions[4]. It is a cheap solution for the long baseline neutrino oscillation experiments at a scale of 100—1000kt, and also applicable to cosmic-ray physics and astrophysics[4]. Reports about these kind of applications can also be found in Ref. [5].

In this paper we report results from a study of a full size prototype, compared with the results from a GEANT4[6]-based full Monte Carlo simulation.

2 Water tank construction

The radiation of Cerenkov light occurs when a charged particle moves through a dispersive medium faster than the group velocity of light in the same medium. Photons are emitted on the surface of a cone, opening at an increasingly acute angle with respect to the particle's momentum direction as the particle slows down. The number of Cerenkov photons generated by the primary particle, dN, is:

$$dN \approx 370(1-1/(n^2\beta^2))dpdx, \qquad (1)$$

For $\beta = 1$, $dN \approx 300$ photons/cm in the wavelength window of $300\text{nm} < \lambda < 600\text{nm}$.

A water tank prototype made of PVC with the dimension of 1m × 1m × 13m is built as shown in Fig. 1. The inner wall of the tank is covered by the Tyevk film 1070D from DuPont. At each end of the tank there is a Winston Cone[7] which can collect parallel

Received 11 April 2005
*Supported by National Natural Science Foundation of China (10225524) and 100 Talents Programme of CAS (U-18)
1) E-mail: mjchen@mail.ihep.ac.cn

light at its focal point, where an 8-inch photomultiplier is installed. The Winston cone is again made of PVC, covered by the aluminium film with protective coating. Cerenkov light produced by through-going charged particles are reflected by the Tyvek and Al film and collected by photomultipliers at the focus of the Winston cone. At the top of the tank there is an air gap (about 1cm) above the water level which serves as a total reflector for photons with certain incident angles.

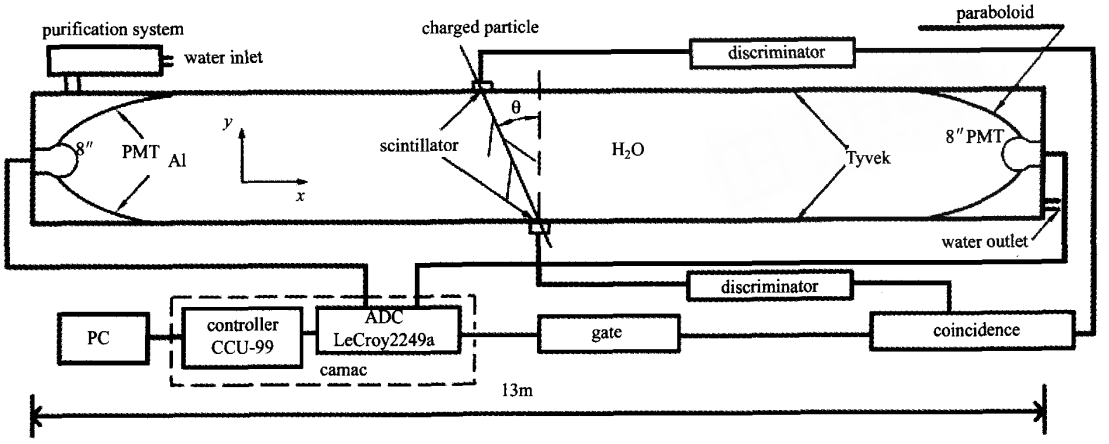

Fig. 1. Schematics of a water tank of the Cerenkov calorimeter. The middle point of the tank is set as the origin of the coordinate system.

Tyevk is a diffuse reflector with a very high reflectivity which is measured in the frequency range of visible light as shown in Fig. 2. Although it is naively believed that mirror reflector such as Al film has a better light collection for such a long optical module, our simulation shows that their performances are actually very similar[8]. The dominant factor is the bulk reflectivity. The good mechanical and chemical properties of Tyvek lead us to use it in order to have an easy handling and less aging effect in the deionized water. Tyvek as a reflector in water has been used by many experiments, including Super-Kamiokande, KamLAND, and Auger experiment[9].

Since the Winston cone needs a mirror reflection to collect light, a selected Al film is used. Al film has a very high reflectivity (98%) in theory, but it is easy to be oxidized in water and lose its reflectivity. A protective coating is hence needed and the reflectivity is measured to be typically 90%, as shown in Fig. 2.

In order to have a good water transparency, clean de-ionized water with a resistance of more than 10MΩ is used. The water is again purified by a simple system with a 0.1μm filter, which can increase the transparency by a factor of two. The water absorption length as a function of wavelength used in Monte Carlo simulation is obtained by scaling down the curve from the Auger experiment[10] based on our experimental data, as shown in Fig. 2. The phototube used is 9350KB from EMI, and its quantum efficiency[11] is shown in Fig. 2.

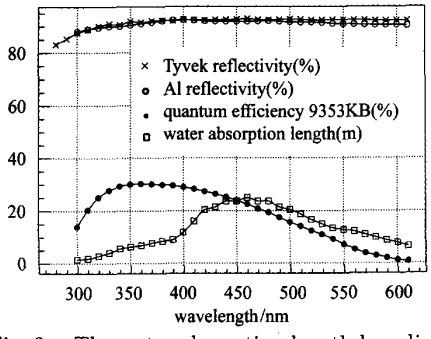

Fig. 2. The water absorption length by adjusting that from Auger experiment, the quantum efficiency of the PMT 9350KB from EMI, and the measured reflectivity of Tyvek and Al as a function of wavelength.

Cosmic-muons, triggered by two scintillator counters at the top and the bottom of the tank, are the primary charged particles which generate Cerenkov photons. The muon flux at the sea level is about $1.8\times10^{-2}/(\mathrm{cm}^2\cdot\mathrm{s})$, and the area of scintillation counters is 20cm×44cm, hence it takes typically 10 hours to accommodate one spectrum. Such a small trigger

counter is selected to control the error due to the incident position, angle and the pass length of muons. A displacement of one of the two trigger counters in x direction(see Fig. 1) can define the incident angle of the muons. In addition, between two runs a calibration run with the trigger counters at $x=0.5$m was taken to monitor the water quality.

The setup also includes a C205 ADC from CAEN to measure the charge of muon and the single photoelectron for calibration, a N844 discriminator from CAEN to generate trigger signals and the gate signal for ADC.

GEANT4 is a C++ toolkit providing the machinery necessary to define the detector geometry and material properties and to simulate particle transport and interactions in the detector materials. Most relevant physics processes have been incorporated, including ionization, delta ray production, multiple Coulomb scattering, bremsstrahlung, and Cerenkov radiation for charged particles. Optical photons produced by processes such as Cerenkov radiation(including Cerenkov radiation from delta rays) may then subject to Rayleigh scattering, absorption, and optical boundary interactions. The reflection and transmission of light at a rough surface is modelled in GEANT4 using a flexible optical model, unified model, to accommodate the main features of both physical and geometrical optical models of surface reflection over a wide range of surface roughness and wavelengths[12]. It allows adjustment of parameters to control the relative contributions of specular reflections from both the average surface normal and the normal of a micro facet at the surface, diffuse(Lambertian) reflection, possible backscattering, and overall surface reflectivity[13].

A GEANT4-based simulation program of the water tank is developed, and proper optical models and parameters of optical surfaces are selected and tested. Since the construction of the water tank is similar in many ways to that of the Auger detector[10], some of the parameter values in our simulation program are very similar[14]. Optical models and their parameters have been discussed in Ref. [8].

3 Results and discussions

3.1 PMT's single-photoelectron spectrum

Single photoelectron spectrum(SPE) is measured before each run in order to calibrate the system since signal amplitudes normalized to that of SPE provide a unique measure of light collected by photomultipliers. SPE can be measured in many ways, one of which is the so-called "thermal noise" method. In total darkness, a photomultiplier can still generate pulses due to thermal emission of single electron by photocathode, equivalent to the charge spectrum of single photoelectron. Thermal emission of electrons by dynodes constitutes the noise below the SPE peak. A SPE spectrum of the PMT 9350KB, applying a high voltage of 1550V at the room temperature(about 15℃), is measured as shown in Fig. 3. Since the ADC used is only 12 bit, the working voltage(1550V) of the PMT is selected to avoid saturation of ADC for cosmic-muons at all positions along the water tank. The SPE spectrum is obtained by a self-trigger with a threshold of 2mV and a gate width of 100ns. The first peak corresponds to the pedestal, the second peak comes from the dynode noise above the 2mV threshold, and the last peak is from SPE, whose position will be used as the normalization to count number of photons. It is clear from the figure that the PMT has a good peak-to-valley ratio of about 1.5 and its noise is small enough.

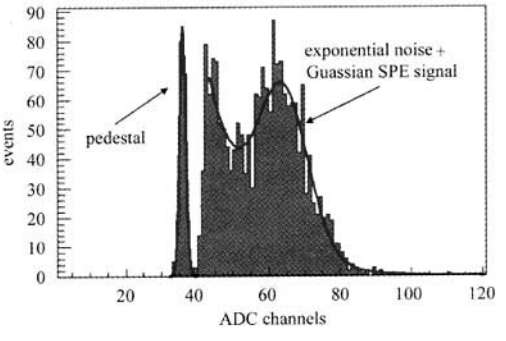

Fig. 3. Single-photon spectrum of the PMT 9350KB at a high voltage of 1550V.

3.2 Position dependent response of the water tank

Light collected for cosmic-muons is a function of distance from the incident point of the muon to the phototube, since the water transparency and reflectivity of the Tyvek film is not perfect. Such a position dependent response of the tank is critical to its energy resolution and pattern recognition capability. Typically it is characterized by an exponential behavior of $e^{-x/\lambda}$, where x is the distance of the muon event to the phototube and λ is the characteristic parameter, often called "effective attenuation length".

The characteristic parameter λ depends on the water transparency, the reflectivity of the Tyvek film, and the geometry of the tank. Fig. 4 shows the charge spectrum collected at $x = 0.5$m with an incident angle of 0°. Using the trigger scintillation counters to define the muon incident location, keeping the y coordinate constant as indicated in Fig. 1, the total light collected as a function of x at several locations is obtained as shown in Fig. 5. An exponential fit yields the measured effective attenuation length of the water tank of (5.74±0.29)m. The line represents the Monte Carlo prediction by adjusting the scale of the water absorption length as shown in Fig. 2, until the effective attenuation length is in agreement with that of the measurement. As what is discussed later, this tuning is justified by the agreement between data and Monte Carlo prediction for both the effective attenuation length and the angular dependent response.

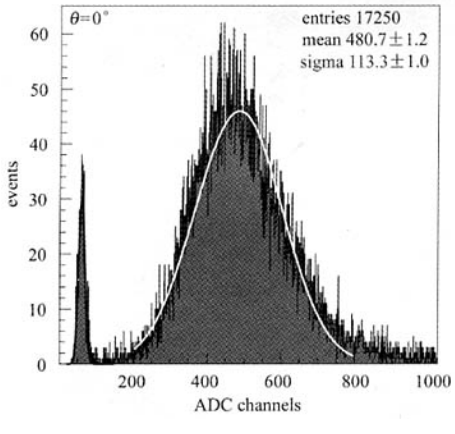

Fig. 4. Charge spectrum collected at $x = 0.5$m with an incident angle of 0°.

It can be seen from Fig. 5 that, for a through-going muons entering the center of the tank, a total of ~20 photoelectrons by each PMT will be collected, corresponding to a statistical fluctuation of about $7\%/\sqrt{E}$. Based on the Monte Carlo simulation, the number of photons at various stages of the photon transport in the water tank is listed in Table 1. From the table, it can be seen that about 74% of light is lost due to the Tyvek reflection and water absorption. The Winston cone has a collection efficiency of 3.1%, the same as the ratio of PMT surface area to that of the water tank cross section. It means that the Winston cone did not improve the light collection efficiency, but the uniformity of the light collection.

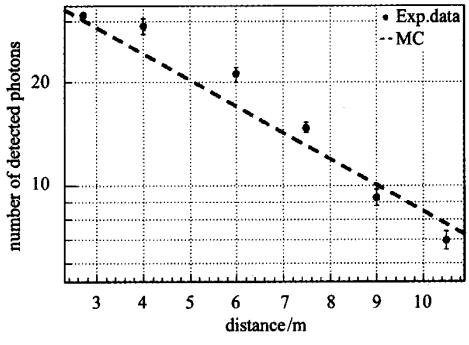

Fig. 5. Position dependent response of the water tank to cosmic-muons. x is the distance from trigger counters to the PMT at right. The line represents the Monte Carlo prediction with an effective attenuation length of 5.79m. The measured effective attenuation length of the water tank is (5.74±0.29)m.

Table 1. Number of photons at various stages of the photon transport in the water tank from Monte Carlo simulation.

No. of Cerenkov photons produced	35156.9±178.7
No. of photons entering Winston cones	9274.4±76.2
No. of photons hitting the glass surface of two PMTs	288.1±18.3
No. of photoelectrons collected by two PMTs	41.5±2.8

There are several ways to improve the light collection of the water tank: (a) The water absorption length can be improved with a more sophisticated purification system. In fact the Super-Kamiokande experiment reached an absorption length of about 90m[15], a factor of 3 better than what was reached here; (b) The reflectivity of the inner liner can be

improved by using the newly-developed plastic reflectors, VM2000 or ESR from 3M Co.[16]. They have a reflectivity better than 99%, which can increase the total light collected by more than 50%. In a word, it is possible to increase the light collection by a factor of two, corresponding to a statistical fluctuation of about $5\%/\sqrt{E}$ for each tank.

3.3 Angular dependent response of the water tank

Since Cerenkov light produced is not isotropic, and its direction is correlated to that of the incident charged particles, the total light collected by phototubes at each end of the water tank is also correlated to the incident angle of the particles. By using trigger counters to define the incident angle as shown in Fig. 1, response of the water tank to through-going charged muons with incident angles varying from 0° to 50° are measured. The bottom trigger scintillator is fixed at $x = 0.5$m, and the top trigger scintillator is moved along the $-x$ direction. After normalizing the track length to 1m, results are shown in Fig. 6(a) together with the predictions from the Monte Carlo simulation. Since the only free parameter to be tuned in the Monte Carlo prediction is the overall scaling of the water absorption length as discussed before, the good agreement between data and Monte Carlo simulation for both the effective attenuation length and the angular dependent response shows that the optical behavior of the water tank is largely understood.

As can be seen from Fig. 6(a), the number of photoelectrons is approximately constant for incident angles less than 30°. This is confirmed by the Monte Carlo simulation, and true at almost all locations of the tank, as shown in Fig. 6(b). This is significant since during the event reconstruction, this factor can be ignored and the energy resolution of neutrino event can be maintained at a reasonably good level. It should be mentioned that the experimental data of the right PMT is only used in the above analysis because the surface of the left PMT was covered by some Tyvek accidently. After the completion of the measurement of effective attenuation length of water, the quality of water had worsened and the calibration runs were taken before each measurement. The data points of Fig. 6(a) is corrected by using calibration runs.

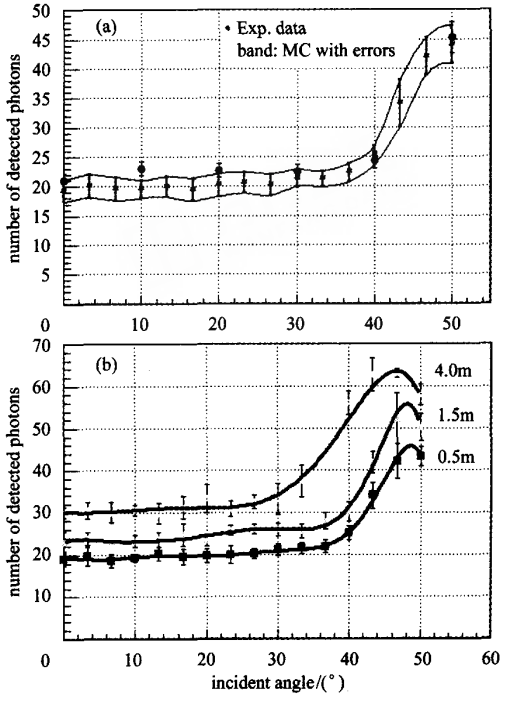

Fig. 6. (a) The measured angular dependent response of the water tank together with the Monte Carlo prediction. The band indicates the statistical error of the Monte Carlo prediction. The track length of all the data points are normalized to 1 meter; (b) The Monte Carlo results of the angular response as a function of distance from the incident point to the phototube.

4 Summary

Water Cerenkov calorimeter is a good candidate for very long baseline neutrino oscillation experiments. A full size water tank prototype, with a dimension of 1m×1m×13m, made of PVC with reflective inner liner was built. The effective attenuation length and the angular response of the tank was measured, and good agreement with a GEANT4-based full Monte Carlo simulation was obtained. The light yield, the total light collection efficiency, the effective attenuation length and the angular dependent response of the tank are all good enough for the long baseline neutrino oscillation experiment, and they can be further improved.

References

1 Fukuda Y et al. Phys. Rev. Lett., 1981, **B81**: 1562
2 Andrew O. Bazarko MiniBooNE: the Booster Neutrino Experiment Presented at DPF99, Los Angeles
3 Becker-szendy R et al(IMB Collaboration). Phys. Rev., 1992, **D46**: 3720
4 WANG Yi-Fang. Proc. of New Initiatives on Lepton Flavor Violation and Neutrino Oscillation with High Intense Muon and Neutrino Sources. Singapore: World Scientific. 242
5 Steinbuegl S, Gebauer J, Lorenz E et al. A New Concept for an Active Element for the Larger Cosmic Ray Calorimeter Ani. Proceeding of ICRC 2001. 912
6 http://geant4.cern.ch/geant4
7 Winston R, Enoch J M. J. Opt. Soc. Amer., 1971, **61**: 1120
8 CHEN M J, ZHANG F, WANG Y F. HEP&NP, 2003, **27**(11): 1015 (in Chinese)
(陈明君, 张峰, 王贻芳. 高能物理与核物理, 2003, **27**(11): 1015)
9 Filevich A, Bauleo P, Bianchi H et al. Nucl. Instrum. Methods, 1999, **A423**: 108
10 Matthiae G. Auger Technical Note GAP-2002-061
11 http://www.electron-tubes.co.uk/pmts/pmt_menu.html
12 Nayer S K et al. IEEE Trans. on Pattern Analysis and Machine Intelligence, 1991, **13**: 611
13 Levin A, Moisan C. TRIUMF Internal Note TRI-PP-96-64. 1996
14 http://www.hep.physics.neu.edu/auger/
15 Choji Saji. Doctoral Thesis. Studying of Upward-Going Muons in Super-Kamiokande, 34
16 MPI-K Progress Report 2001/2002, 43; VikuitiTH ESR Brochure, http://www.3m.com

水基切伦科夫量能器模型的研究*

陈明君[1,2;1)] 王贻芳[1] 何景棠[1] 孟祥承[1] 俞梅凌[1] 杨长根[1] 曹俊[1]

1 (中国科学院高能物理研究所 北京 100049)
2 (中国科学技术大学 合肥 230026)

摘要 为了研究极长基线中微子振荡, 构造了一个大小为1m×1m×13m水基切伦科夫量能器模型. 测量得到的水箱的有效衰减长度为(5.74±0.29)m, 并且研究了光的收集能力随入射粒子角度变化的关系. 同时发展了基于GEANT4软件包, 包含有详细的光学过程的模拟程序, 所得到的模拟结果与实验测量有很好的一致性. 说明水箱可以作为水基切伦科夫量能器的可行性的方案.

关键词 中微子 振荡 探测器 量能器

2005 – 04 – 11 收稿
*国家自然科学基金(10225524)和中国科学院百人计划(U-18)资助

1) E-mail: mjchen@mail.ihep.ac.cn

水基切伦科夫量能器模型的研究

作者： 陈明君， 王贻芳， 何景棠， 孟祥承， 俞梅凌， 杨长根， 曹俊， CHEN Ming-Jun， WANG Yi-Fang， HE Jing-Tang， MENG Xiang-Cheng， YU Mei-Ling， YANG Chang-Gen， CAO Jun

作者单位： 陈明君,CHEN Ming-Jun(中国科学院高能物理研究所,北京,100049;中国科学技术大学,合肥,230026)， 王贻芳,何景棠,孟祥承,俞梅凌,杨长根,曹俊,WANG Yi-Fang,HE Jing-Tang,MENG Xiang-Cheng,YU Mei-Ling,YANG Chang-Gen,CAO Jun(中国科学院高能物理研究所,北京,100049)

刊名： 高能物理与核物理 ISTIC SCI PKU

英文刊名： HIGH ENERGY PHYSICS AND NUCLEAR PHYSICS

年，卷(期)： 2005，29(10)

引用次数： 0次

参考文献(17条)

1. Fukuda Y 查看详情 1981

2. Andrew O Bazarko MiniBooNE:the Booster Neutrino Experiment Presented at DPF99,Los Angeles

3. Becker-szendy R 查看详情 1992

4. WANG Yi-Fang Proc.of New Initiatives on Lepton Flavor Violation and Neutrino Oscillation with High Intense Muon and Neutrino Sources

5. Steinbuegl S.Gebauer J.Lorenz E A New Concept for an Active Element for the Larger Cosmic Ray Calorimeter Ani

6. 查看详情

7. Winston R.Enoch J M 查看详情 1971

8. 陈明君.张峰.王贻芳 查看详情[期刊论文]-高能物理与核物理 2003(11)

9. Filevich A.Bauleo P.Bianchi H 查看详情 1999

10. Matthiae G Auger Technical Note GAP-2002-061

11. 查看详情

12. Nayer S K 查看详情 1991

13. Levin A.Moisan C TRIUMF Internal Note TRI-PP-96-64 1996

14. 查看详情

15. Choji Saji Doctoral Thesis.Studying of Upward-Going Muons in Super-Kamiokande

16. MPI-K Progress Report 2001/2002

17. VikuitiTH ESR Brochure

相似文献(10条)

1. 期刊论文 何景棠.He Jingtang 中微子质量和中微子振荡实验 -物理学进展2001,21(2)

本文介绍中微子质量测量的历史和现状。介绍太阳中微子丢失实验的结果和大气μ中微子丢失实验结果。这些结果表明存在中微子振荡，即中微子具有质量。它是超出标准模型的信号。本文还介绍了21世纪初研究中微子振荡的若干重要实验，例如长基线中微子振荡实验以及建造μ子贮存环来产生高能电子中微子束进行中微子振荡的实验以及测量中微子振荡时的CP破坏的设想。

2. 期刊论文 王较过.WANG Jiao-Guo 中微子振荡与中微子的静止质量 -物理2000,29(11)

简要回顾了中微子的发现过程，论述了中微子的 基本性质及三种不同类型的中微子，讨论了中微子振荡的最新实验结果及其与中微子静止质 量的关系，指出了中微子的静止质量在物理学与天文学中的重要性以及确定中微子的静止质 量有待进一步解决的问题.

3. 学位论文 陈伯伦 中微子实验和振荡参数分析的若干研究 2008

宇宙大爆炸初期，中微子已经大量的存在了。由于中微子本身质量非常小，不带电，只参加弱相互作用，反映截面非常小，因此，大量的中微子长时间的存留下来。除了大爆炸后遗留下来的中微子，宇宙中还存在广泛的中微子产生源，例如超新星爆发，恒星内部核反应，宇宙射线以及地球上各种物质的衰变过程等。但是由于与物质的作用截面非常小，中微子的探测非常困难，因此我们对中微子的认识仍然很肤浅。自从Pauli提出中微子假说至今已经有70多年的时间了，中微子依然是萦绕在科学家头脑中的难题。

现在我们知道存在三代中微子，最早电子味的中微子在1956年通过反应堆实验被探测到。而放射性化学实验Homestake对太阳产生的电子味中微子进行探测，发现电子味中微子在传播到地球的过程中发生了缺失现象。随后进行的一系列实验均证实了这一结论。对此存在很多可能的解释，其中一种可能的解释就是中微子振荡机制，也就是电子味中微子在从太阳传播到地球的过程中转换成了其他味的中微子。先期的实验只能证实探测器探测到的中微子比理论预期的少，还不能确定这是否是由于中微子振荡引起的。太阳中微子问题的真正突破是在2001年后，新一代的太阳中微子实验SNO通过1000吨重水同时测量三种味的中微子，从而获得了电子味中微子的消失以及 ν<,μ>， ν<,τ>的产生证据，而且三种中微子的总流量与John Bahcall给出的标准太阳模型的预言是一致的。虽然其他的解释还不能完全排除，但是中微子振荡机制是对太阳中微子问题最自然，最可能的一种解释。而此后进行的反应堆中微子实验KamLAND，第一次探测到40％的反应堆中微子消失了。这最终确认了中微子振荡机制。现在可以肯定地说，太阳中微子发生了振荡，转换为了其他味的中微子，而且太阳中微子混合是大角度混合。中微子是有质量的。这有着重要的意义，它要求修改粒子物理的标准模型，预示着存在超出标准模型的新物理，如轻子数不守恒，质子衰变等。中微子物理成为近年来科学研究的一个重要方向。

中微子是一种极为神秘的粒子，自从发现中微子振荡以后，可以说它的神秘面纱已逐渐被揭开。研究中微子物理，一个重要的方向就是分析中微子实验，应用中微子振荡机制给出中微子参数的区间估计。我们首先回顾了粒子物理中中微子质量的描述，给出Dirac质量，Majorana质量以及更为一般的Dirac-Ma2iorana质量的表述形式。然后对中微子振荡进行了详尽的讨论，得出了两味中微子的简单情况下，真空和物质中的振荡生存几率。并主要讨论了均匀物质和绝热近似下的振荡公式以及物质效应引起的MSW共振机制。我们应用中微子振荡机制来解释太阳中微子实验，使用了传统的最小方差分析以及贝叶斯分析方法，对中微子实验数据进行了分析，从而给出了太阳中微子问题的LMA MSW绝热解的参数区间。利用贝叶斯方法的独特性质，我们还排除了中微子振荡的一些其他模型，很好的验证了LMA解，并且证明现在的LMA解已经非常稳定和可靠。另外，通过太阳中微子实验的分析和大气中微子实验的结果，轻子混合矩阵PMNS的6个独立参数中，我们已经知道了四个，还有两个是未知的，其中包括了最重要的CP破缺相因子。由于混合矩阵中CP相因子都是与θ<,13>耦合在一起的，因此实验对θ<,13>的测量变得尤为重要。只有完成对θ<,13>的测量，才能开始至关重要的寻找CP破坏效应及其根源的实验研究。因而θ<,13>的探测对研究味物理的核心问题意义重大。一旦θ<,13>被测定，将极大地提高我们对太阳、大气和长基线中微子振荡次级效应的认识，也将有助于我们研究超新星中微子振荡问题。位于中国广东的大亚湾反应堆中微子实验有可能会对θ<,13>进行很好的测量。我们使用不同的分析方法，对大亚湾中微子实验的不同方案进行了模拟，并给出了一个我们认为更为有效的探测器摆放方案，在我们的模拟中，大亚湾中微子实验有希望探测到sin<’2> 2θ<,13>大于0.02的值。大亚湾实验有着非常好的实验条件，在技术上没有太多的困难，是非常可行的反应堆中微子实验，随着实验技术的发展，大亚湾实验还有可能取得比我们模拟更精确的结果。中微子研究是当前粒子物理，天体物理和宇宙学研究的前沿热点。近年来中微子物理研究的一系列重大成果预示着粒子物理研究的新突破。中微子物理正处于一个大发展时期。中微子是最轻的基本粒子，是所有粒子衰变的最终产物。中微子有微小的质量，使得它可以构成宇宙中的热暗物质，对宇宙结构的形成有重要的影响。中微子振荡中的CP破缺可能对理解宇宙中的物质反物质不对称现象起关键作用。同时，中微子携带天体的许多信息，中微子不带电，不会像带电粒子一样被物质阻挡和磁场偏转，也不会像光子和带电粒子一样，与宇宙背景辐射相互作用。因此用中微子作探针，可以直达宇宙深处，将极大地推动天文学的发展。中微子振荡生存几率与其通过的物质密度有关，因此用中微子作探针，还能测量中微子通过地段的物质密度，从而获得太阳，地球的内部信息。随着科学的发展，我们会对中微子有更多的了解和认识。

4.期刊论文 何景棠.HE Jing-Tang 中微子振荡实验——超出标准模型的实验检验(Ⅰ) -物理2001,30(2)

文章总结了中微子振荡实验的历史和现状.介绍了几个太阳中微子丢失实验的结果和几个大气μ中微子丢失实验结果.这些结果表明存在中微子振荡，即中微子具有质量.它是超出标准模型的信号.文章还介绍了21世纪初研究中微子振荡的若干重要实验，例如长基线中微子振荡实验以及建造μ子贮存环来产生高能电子中微子束进行中微子振荡的实验以及测量中微子振荡时的CP破坏的设想.

5.期刊论文 叶子飘.胡宝坚 中微子振荡与太阳中微子问题 -湖南大学学报(自然科学版)2002,29(1)

认为太阳中微子问题主要是标准太阳模型没有考虑7Be(3He,p)9B核反应道的竞争,并且在计算7Be中微子和pep中微子时,并没有考虑到太阳电子温度与离子温度的差异.如果考虑了这种差异,则太阳中微子问题可以得到很好地解决,而不需要修改太阳的其它重要参数.

6.学位论文 黄秀菊 引力场中的质量中微子振荡 2006

中微子是基本粒子家族中重要且具有特色的成员之一，是唯一只参与弱相互作用的粒子，它在理论物理学及天体物理学中都占有着十分重要的地位。

泡利提出中微子假说之后，人们进行了一系列捕获中微子的实验。现在这些实验都用无可辩驳的事实证明了中微子是客观存在的基本粒子，同时也促使人们从多方面对中微子进行深入的研究。其中中微子的质量问题和中微子振荡现象是研究的热门课题。在费米弱作用理论乃至弱电统一理论中，都是把中微子当作无静止质量的粒子来处理的。用这样的理论来计算各种物理过程中的结果，都与实验符合得很好。另一方面，如果中微子质量不为零，则可很自然地解释某些现象(如宇宙中的热暗物质问题，太阳中微子丢失问题等)。于是一些理论也试图赋予中微子以质量，同时人们也在用不同的方法来测量和计算中微子的质量。虽然随着实验技术的飞速发展，实验测量到的中微子质量上限值不断下降，但目前各种实验还未精确确定中微子的质量值。

另外，早在1958年，Pontecorvo就指出，如果中微子质量不为零，则不同种类的中微子之间可能会相互转化，即产生中微子振荡现象。由中微子振荡的量子力学可知，在探测点发现一种中微子转化为另一种中微子的振荡几率与混合角、中微子束的平均能量、中微子产生源一探测器间的距离以及两种中微子的质量平方差有关。本文在此基础上主要讨论中微子振荡的干涉相因子以及中微子振荡中的CP破坏效应。因此，本文的结构安排如下：

在第一章的引言中，介绍了中微子的发现、中微子的质量、以及中微子的混合和振荡现象，然后在此基础上，用量子力学的语言描述了中微子的振荡。

在第二章中，介绍了平直时空中的中微子振荡，得到了中微子振荡的干涉相因子。并且指出此因子与中微子束的平均能量、两种中微子质量平方差以及中微子产生点到探测点间的距离有关。

在第三章中，借助于短程线，讨论了爱因斯坦引力理论下的质量中微子振荡。首先利用标准方法讨论了Schwarzschild时空中中微子振荡干涉的相因子，然后用同样的方法分别讨论了Reissner-Nordstr(o)m(R-N)场和Kerr场中的干涉相因子。由结果可知，虽然R-N场源的电荷和Kerr场源旋转的角动量的存在会对相因子的表示结果有贡献，但与Schwarzschild场中的情况相比，此贡献对相因子的增加很小。本章最后，本文给出了Robertson-Walker(R-W)场中中微子振荡的干涉相因子。

在第四和第五章中，分别在Brans-Dicke(B-D)引力理论和有挠引力理论中的静态球对称时空中计算了中微子振荡的干涉相因子。在B-D引力理论框架下得到对干涉相因子明显的贡献，这可以作为一个B-D理论有效性的检验公式。而在有挠引力理论下得出的对真空相因子的修正在某些条件下比广义相对论对相因子的修正要大一些，但前者依然很小。因此中微子振荡实验不能提供一个证据来判断哪一个引力理论更好，广义相对论或是其它引力理论。

在第六章中，介绍了电荷共轭(C)与宇称(P)联合操作对称性的破坏(CP破坏)。接着给出了直接CP破坏的理论研究和实验验证，CP破坏机制和新的CP破坏源。然后在此基础上，讨论了中微子振荡中的CP破坏效应，从中得出：在2味中微子振荡中，混合矩阵是实的，不存在CP破坏；但在3味中微子振荡中，由于混合矩阵不是实的，这直接导致CP对称性的破坏。

7.期刊论文 焦善庆.张金伟.郝军.张晓红 大气中微子νμ振荡几率估算 -益阳师专学报2000,17(5)

据高能中微子的"长基线"实验计设参数,用数值实验常数相关联的唯象方法算出中微子质量数值,估算了中微子振荡几率,判断了μ中微子νμ与τ型中微子ντ最可能发生振荡.

8.期刊论文 焦善庆.张金伟.郝军.张晓红 大气中微子νμ振荡几率估算 -益阳师专学报2000,17(5)

据高能中微子的"长基线”实验计设参数,用数值实验常数相关联的唯象方法算出中微子质量数值,估算了中微子振荡几率,判断了μ中微子νμ与τ型中微子ντ最可能发生振荡.

9.学位论文 陈明君 中微子水基契伦可夫量能器的研究 2006

近十年来，中微子物理不断的获得突破，它已经成为最前沿的物理方向之一。而长基线中微子振荡实验具有丰富的物理内容，可以精确地测量中微子振荡参数，例如sin22θ13，中微子在物质中的效应，质量平方差，CP破坏相角δ等。基于此目的，我们构建了一个全尺寸(1m×1m×13m)的水基契伦可夫量能器模型，验证了它所组成的大型探测器可以用于长基线中微子振荡实验的远端探测器。

第一章中，简单叙述了中微子物理的发展历史，并讨论了中微子真空振荡理论和物质中的振荡理论。提及了可以验证中微子振荡的一些太阳中微子实验和大气中微子实验，得到了MNSP矩阵中的部分参数值。由此提出长基线中微子振荡实验，论及它所能测量的物理目标和一些长基线中微子振荡实验

的未来发展状况。

在第二章，详细论述了所构建的水基契伦可夫量能器模型。首先，分析了已知的一些用于长基线中微子振荡实验的探测器类型，比较得出我们构造的探测器所具有的优点。对所构造的水基契伦可夫量能器的单个模型的论述，包括了量能器的结构，反射材料的筛选，光电倍增管的性能研究，电子学系统，以及净化系统等。

第三章，则论及GEANT4工具包和基于此的单个水箱模拟程序G4WT。GEANT4是最近几年发展的用于高能物理研究的非常有效的模拟工具包，其中论及了G4WT模拟程序中的重点内容：GEANT4的光学过程描述。分析了G4WT模拟程序的框架结构，时间性能等。

第四章则包括了对水基契伦可夫量能器模型的具体测量。详细论述了实验的内容和过程，对于在水箱中不同位置和不同角度的取数，得到了水基契伦可夫量能器的水的有效衰减长度，和契伦可夫光的探测效率的角度依赖关系。最后，还述及了实验中一些不是理想的结果和讨论。

最后一章中，利用第四章的实验结果，结合G4WT模拟程序和基于GEANT3的模拟程序WCC的方法，以及采用了Minos的中微子产生子，基于H2B实验设想的背景，对于水基契伦可夫量能器的能量重建能力，背景等性能作了深入的分析和探讨。

本篇论文完整的描述了一个用于长基线中微子振荡实验的探测器模型。论证了该量能器的光产额，总的探测效率，水的有效衰减长度和粒子入射角度依赖关系都能很好的满足极长基线中微子振荡实验。通过模特卡罗模拟可知，它将是长基线线中微子振荡实验一个非常优秀的探测器的候选者。

10.期刊论文 肖鸿飞 在中微子振荡中的CP破坏 -原子与分子物理学报2003,20(3)

讨论了中微子味混合与中微子振荡的理论,定量地研究了在中微子振荡中的CP破坏效应.在一类超对称模型中,计算了真空中中微子振荡几率和 CP破坏效应.